

Supporting Information for:

Importance of Optimal Composition in Random Terpolymer Based Polymer Solar Cells

*Tae Eui Kang,^a Han-Hee Cho,^a Hyeong-jun Kim,^a Wonho Lee,^a Hyunbum Kang,^a and
Bumjoon J. Kim^{a,*}*

^a Department of Chemical and Biomolecular Engineering, Korea Advanced Institute of
Science and Technology (KAIST), Daejeon 305-701, Korea

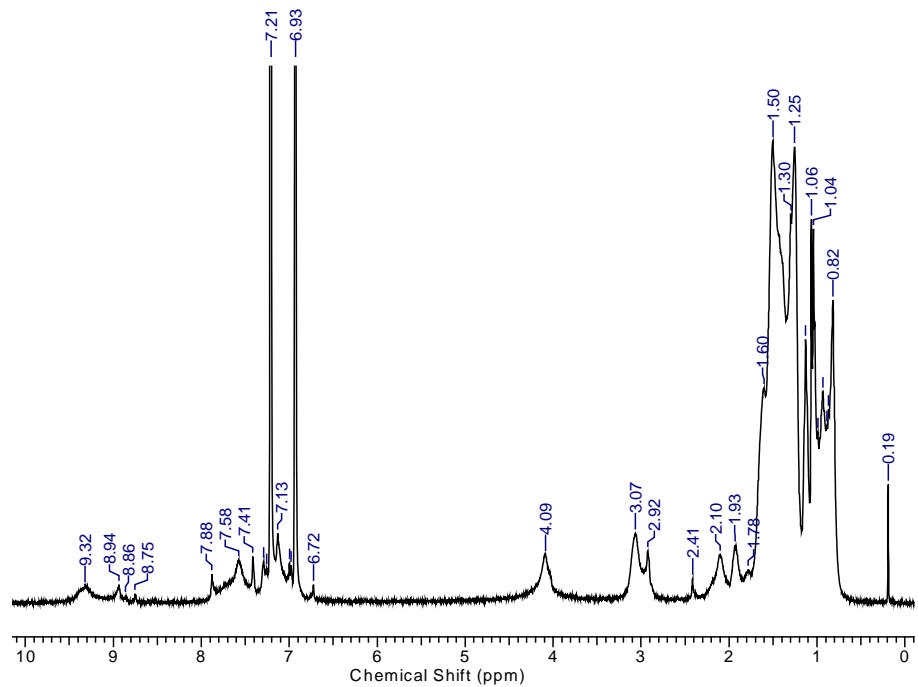
*Electronic mail: bumjoonkim@kaist.ac.kr

Table of contents

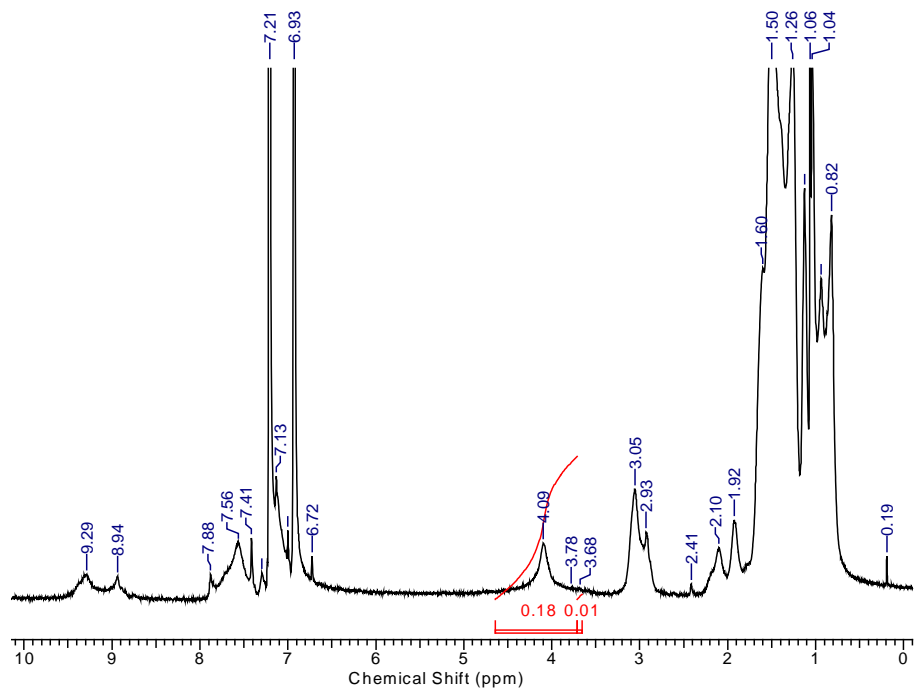
Supplementary Figures S1-10

■ ¹ H NMR of copolymers (P1-P7)	S1
■ TGA plots of P1-P7 with a heating rate of 10 °C /min under nitrogen	S2
■ UV-vis absorption spectra for P1-P7 in thin films	S3
■ CV curves of P1-P7 with an Ag quasi-reference electrode	S4
■ SCLC <i>J-V</i> characteristics of P1, P3, P4, P5 , and P7	S5
■ <i>J-V</i> characteristics of P2 and P6	S6
■ The calculated HOMO and LUMO orbitals for (BDTT-DPP) ₃ and (BDTT-TPD) ₃	S7
■ GIXS patterns of pristine films of P1, P3, P4, P5 , and P7	S8
■ TEM images of P1 and P5 films blend with PCBM.	S9
■ EQEs of PSCs based on P1-P7 devices	S10

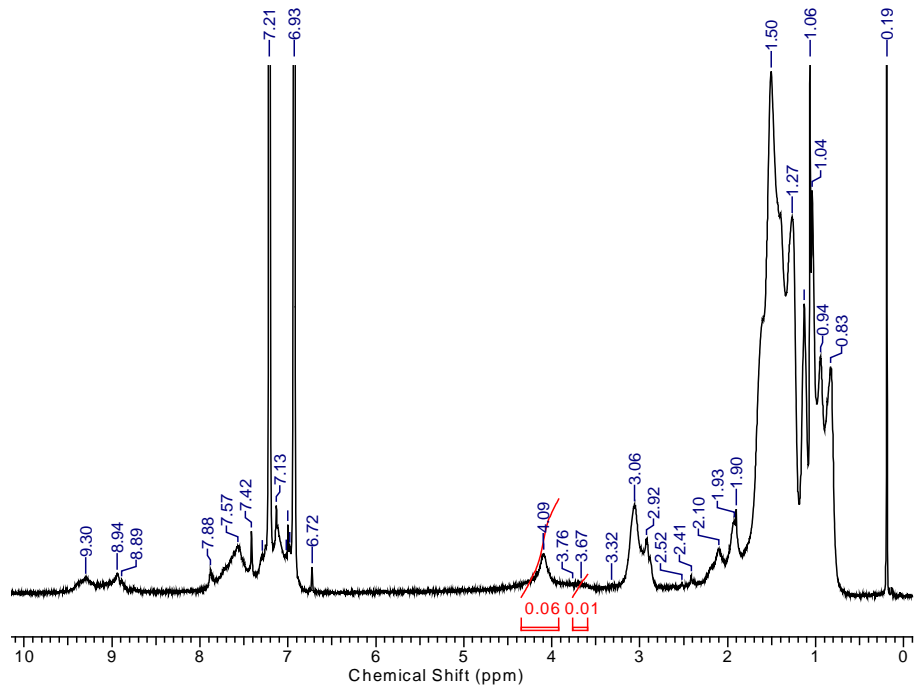
(a) PBDTT-DPP100 (**P1**)



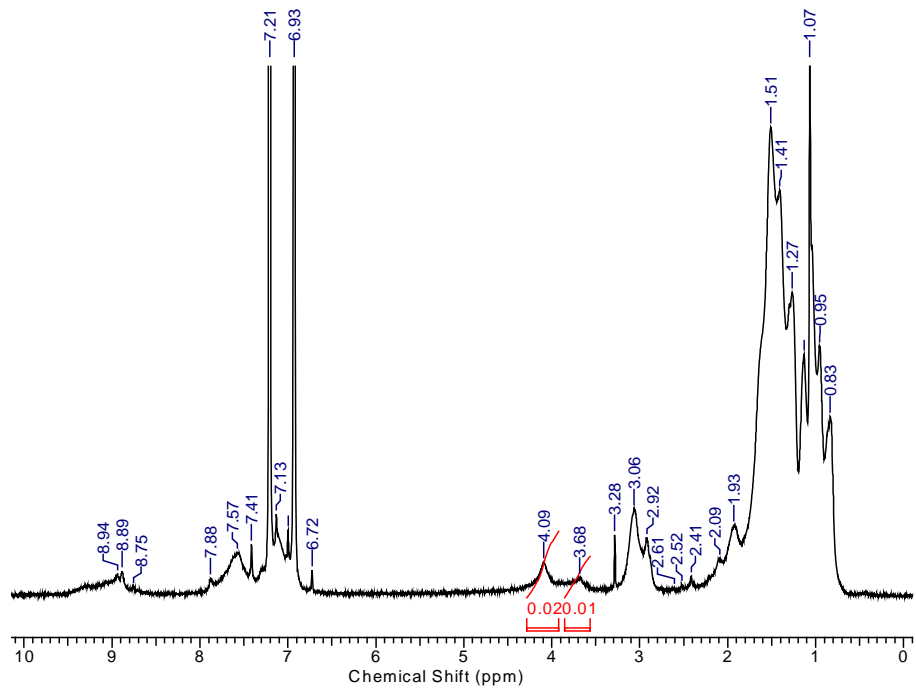
(b) PBDTT-DPP90-TPD10 (**P2**)



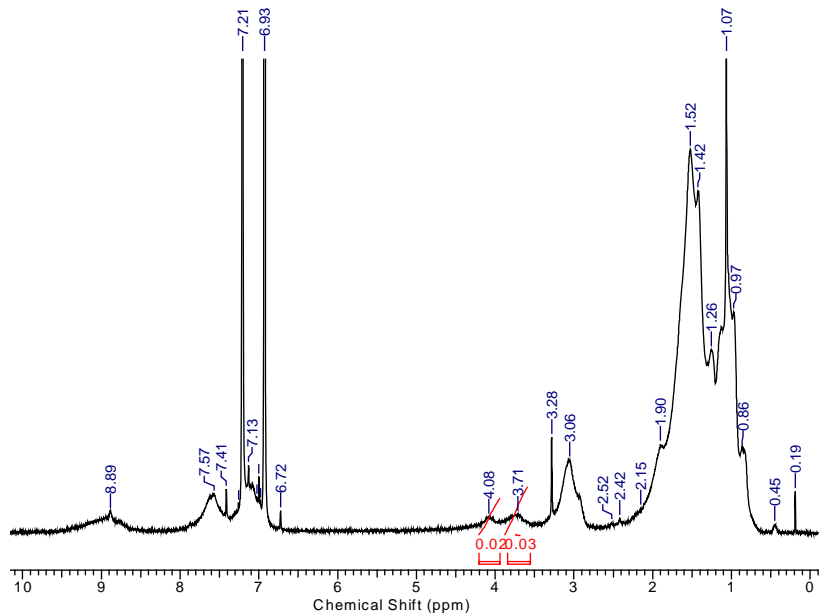
(c) PBDTT-DPP75-TPD25 (**P3**)



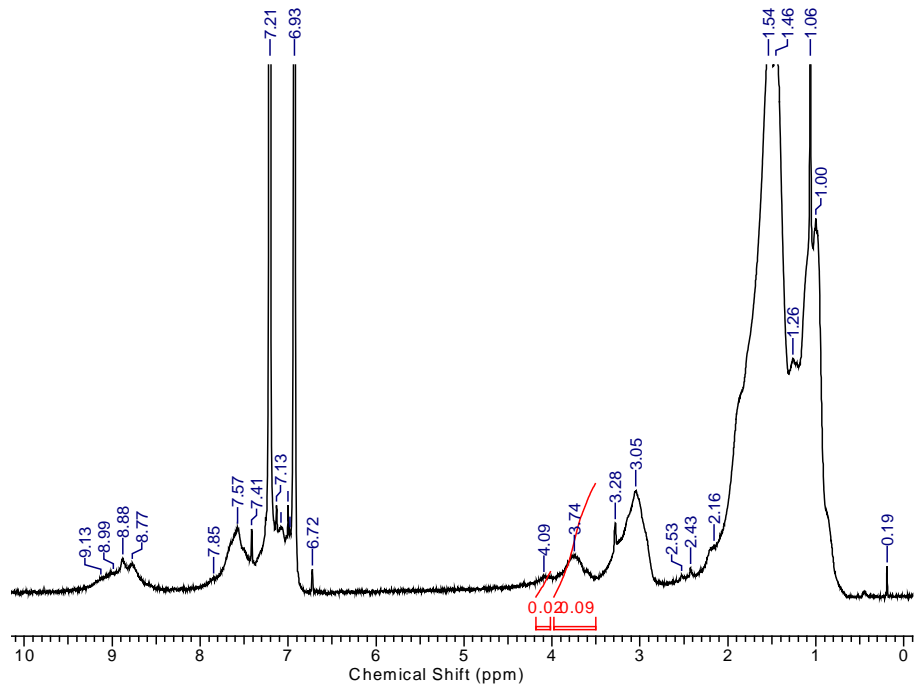
(d) PBDTT-DPP50-TPD50 (**P4**)



(e) PBDTT-DPP25-TPD75 (**P5**)



(f) PBDTT-DPP10-TPD90 (**P6**)



(g) PBDTT- TPD100 (**P7**)

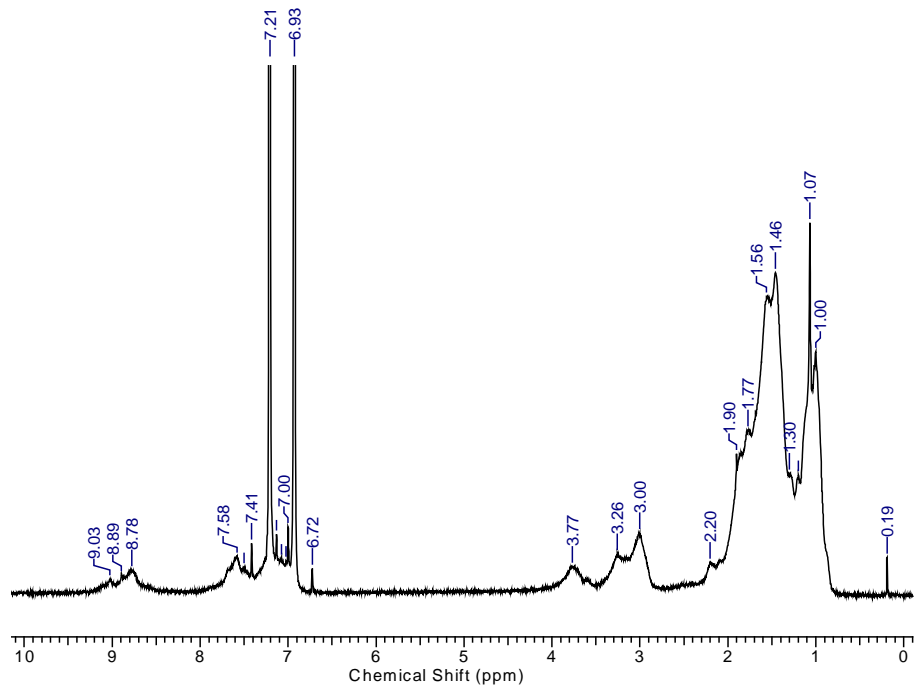


Figure S1. ¹H NMR of (a) PBDTT-DPP100 (**P1**), (b) PBDTT-DPP90-TPD10 (**P2**), (c) PBDTT-DPP75-TPD25 (**P3**), (d) PBDTT-DPP50-TPD50 (**P4**), (e) PBDTT-DPP25-TPD75 (**P5**), (f) PBDTT-DPP10-TPD90 (**P6**), and (g) PBDTT-TPD100 (**P7**).

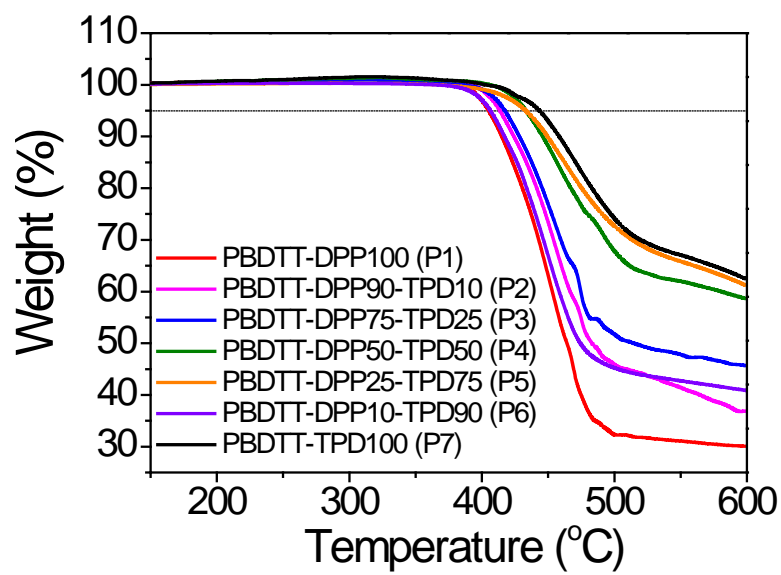


Figure S2. TGA plots of **P1-P7** with a heating rate of 10 $^{\circ}\text{C}/\text{min}$ under nitrogen.

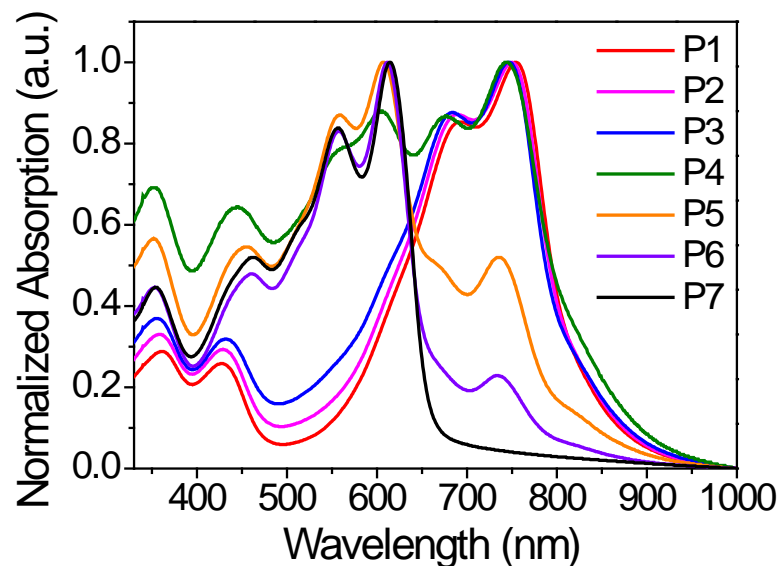


Figure S3. UV-vis absorption spectra for **P1-P7** in thin films.

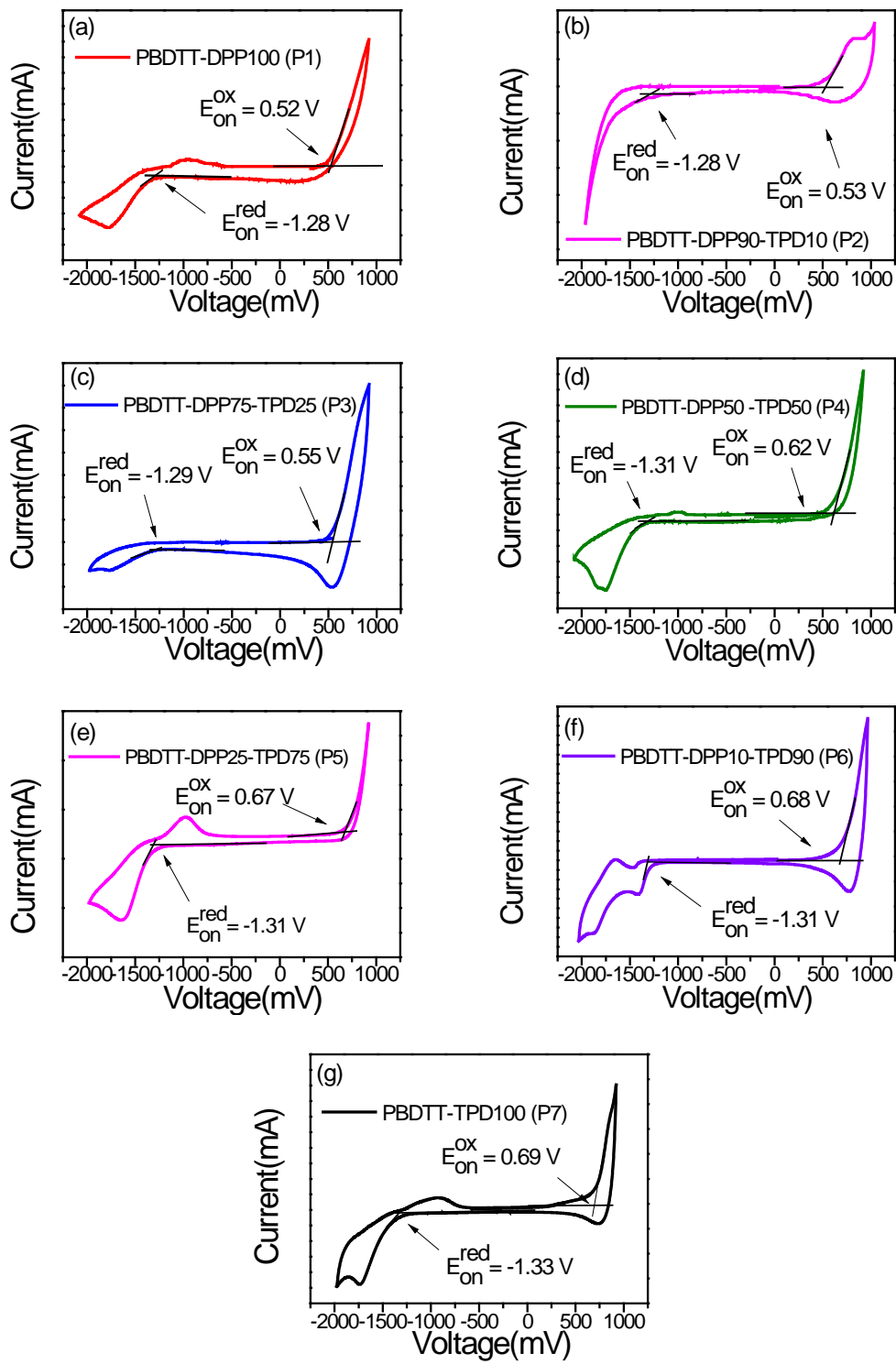
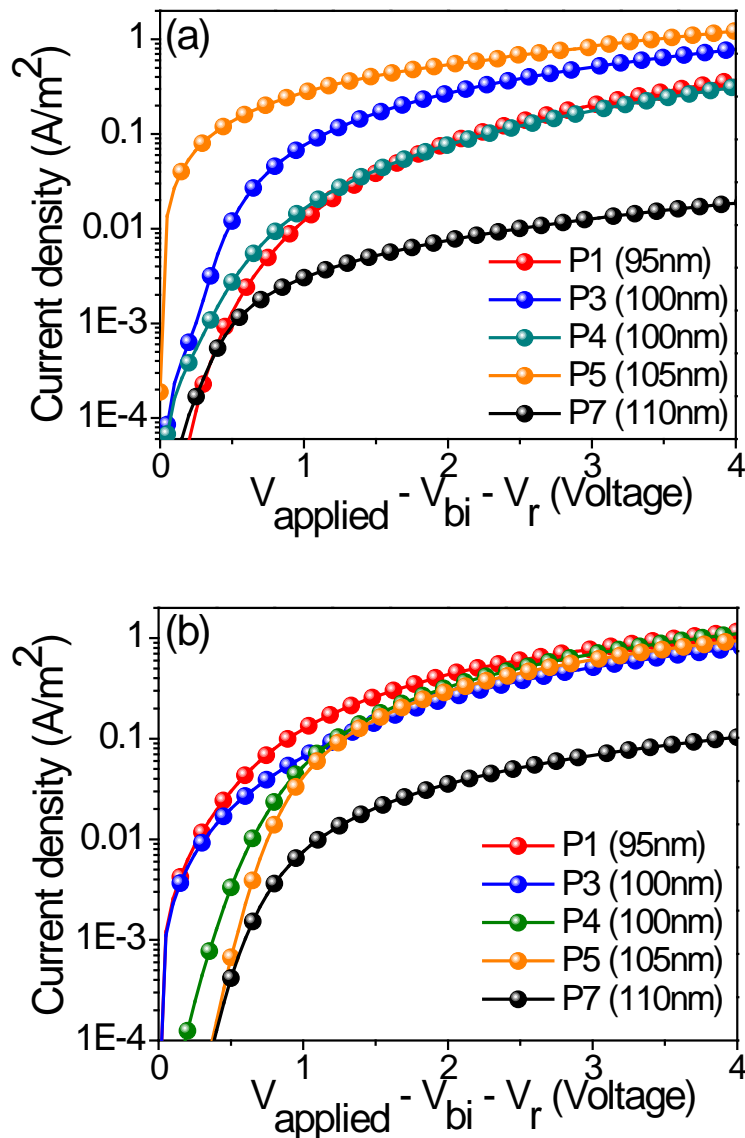


Figure S4. Cyclic voltammograms of (a) PBDTT-DPP100 (**P1**), (b) PBDTT-DPP90-TPD10 (**P2**), (c) PBDTT-DPP75-TPD25 (**P3**), (d) PBDTT-DPP50-TPD50 (**P4**), (e) PBDTT-DPP25-TPD75 (**P5**), (f) PBDTT-DPP10-TPD90 (**P6**), and (g) PBDTT-TPD100 (**P7**).



	P1	P3	P4	P5	P7
Hole mobility ($\text{cm}^2/\text{V}\cdot\text{s}$)	1.14×10^{-4}	1.13×10^{-4}	1.09×10^{-4}	1.10×10^{-4}	1.18×10^{-5}
Electron mobility ($\text{cm}^2/\text{V}\cdot\text{s}$)	1.24×10^{-4}	1.13×10^{-4}	1.76×10^{-4}	1.34×10^{-4}	2.82×10^{-5}

Figure S5. Measured space-charge-limited J - V characteristics of the **P1**, **P3**, **P4**, **P5**, and **P7** blends with PC₇₁BM (or PC₆₁BM) devices under dark conditions (a) for hole-only devices (b) for electron-only devices.

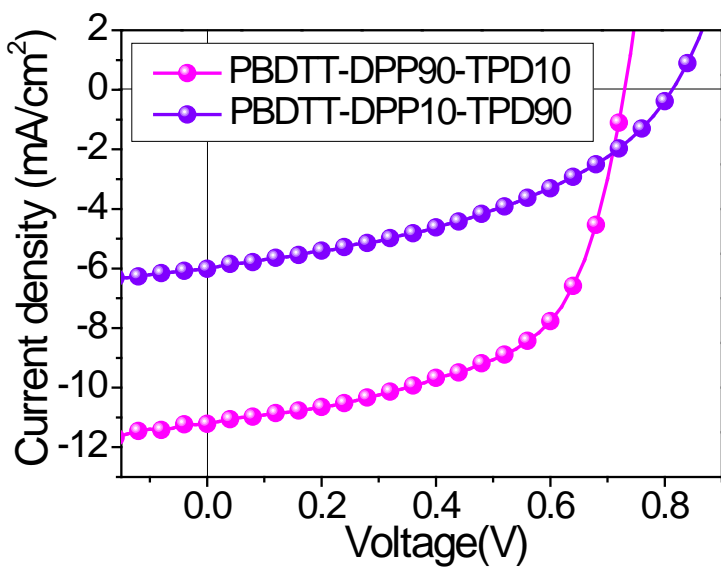


Figure S6. *J-V* characteristics of PBDTT-DPP90-TPD10 (**P2**):PC₇₁BM and PBDTT-DPP10-TPD90 (**P6**):PC₆₁BM.

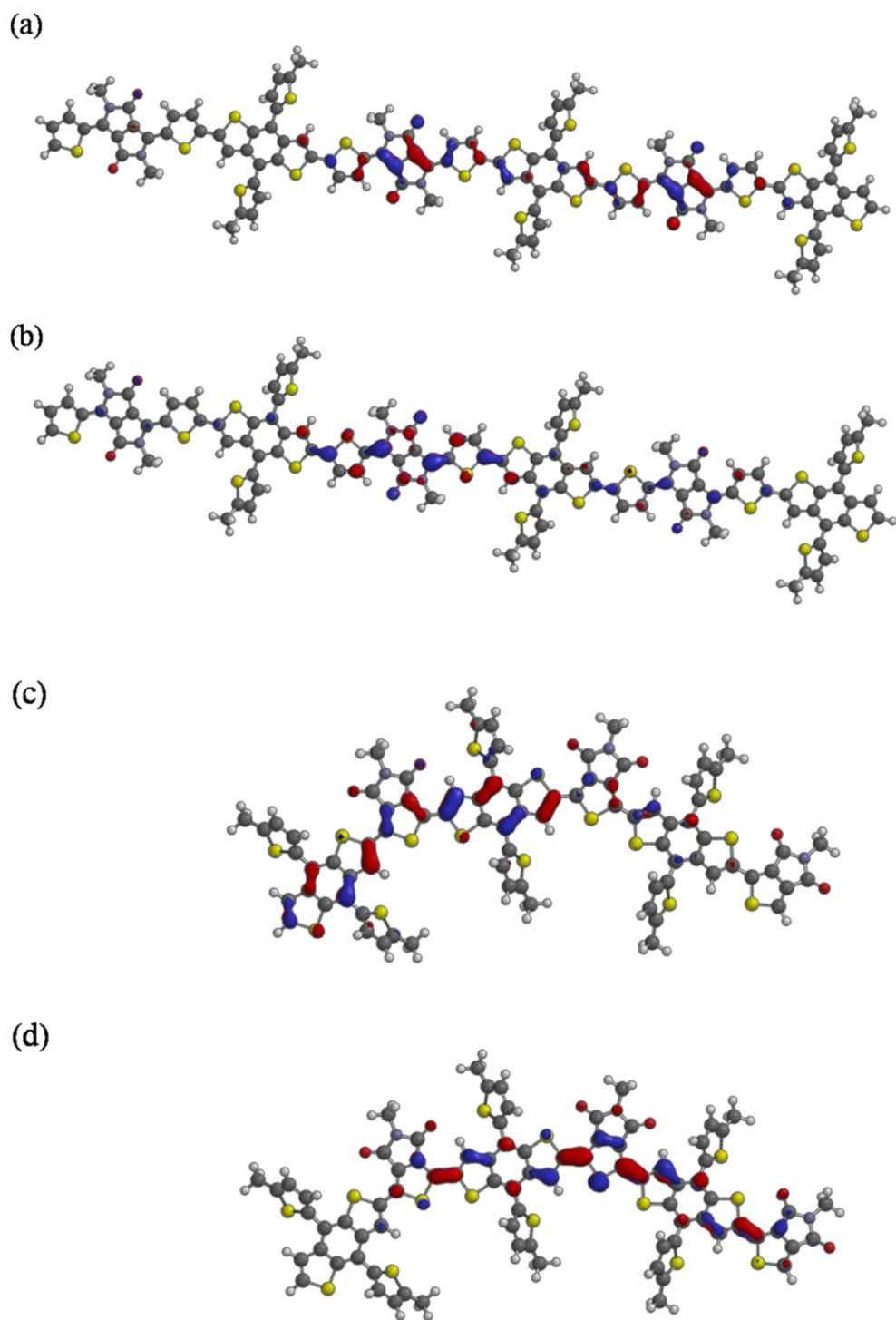


Figure S7. Calculated HOMO and LUMO orbitals for **(BDTT-DPP)₃** ((a) and (b)) and **(BDTT-TPD)₃** ((c) and (d)).

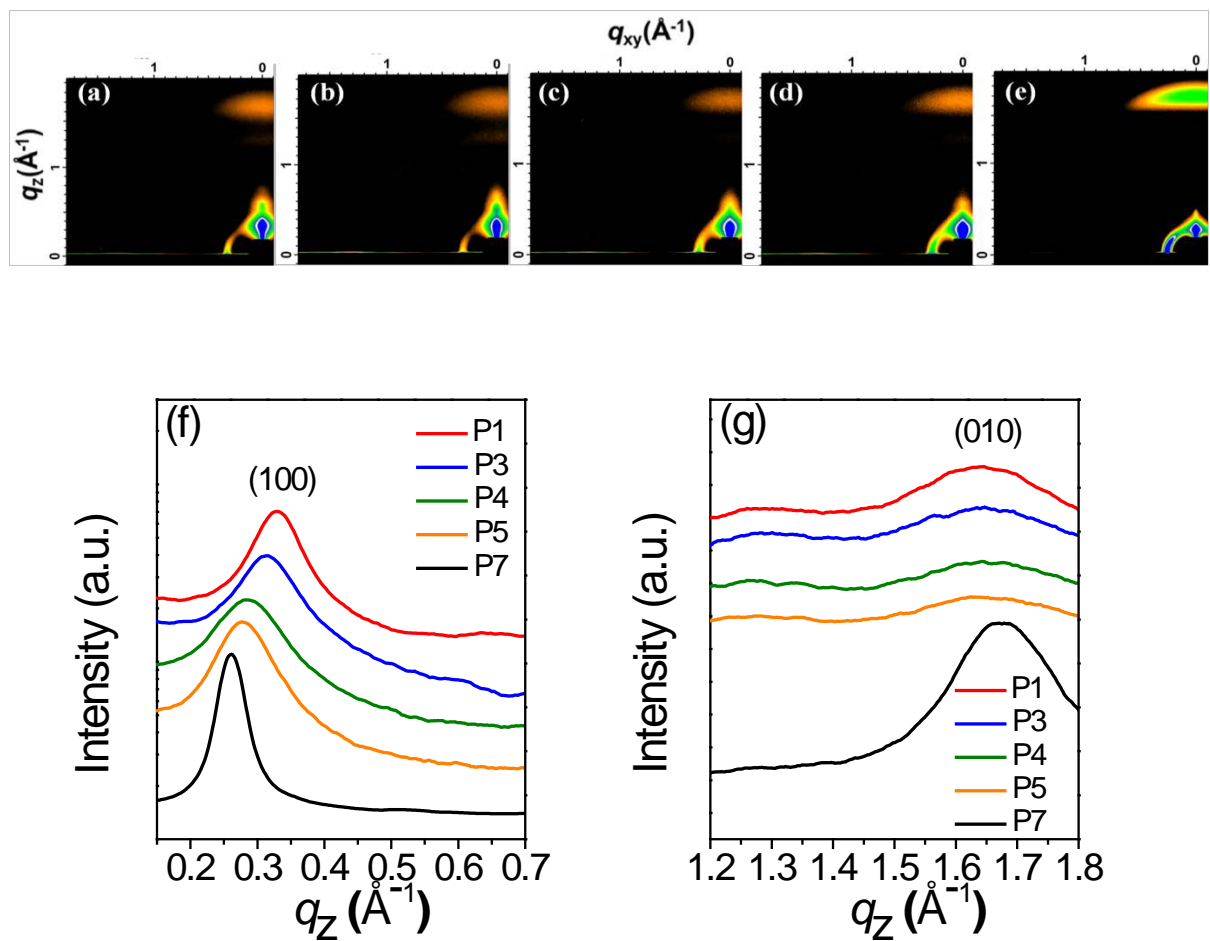


Figure S8. GIXS patterns of pristine films of (a) **P1**, (b) **P3**, (c) **P4**, (d) **P5**, and (e) **P7**. (f) In-plane line and (g) out-of-plane line cuts of GIXS.

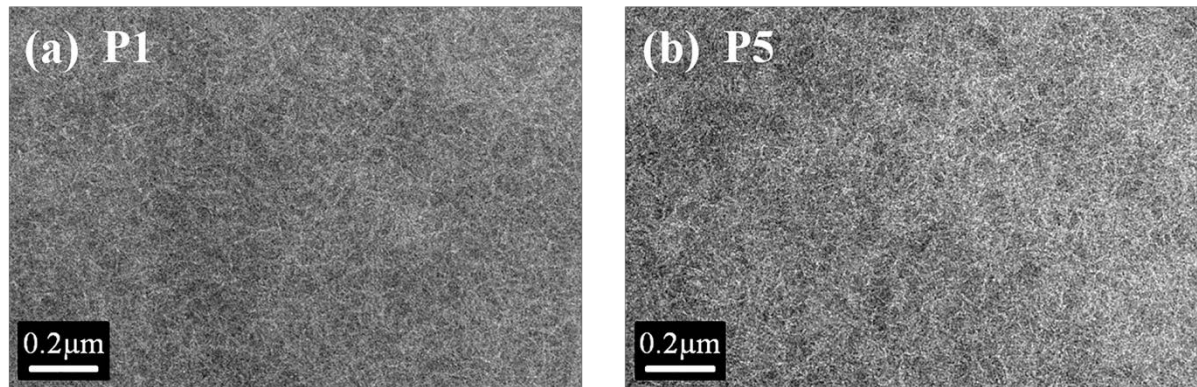


Figure S9. TEM images of the blend films of (a) PBDTT-DPP100 (**P1**) and (b) PBDTT-DPP25-TPD75 (**P5**). The scale bar is 200 nm.

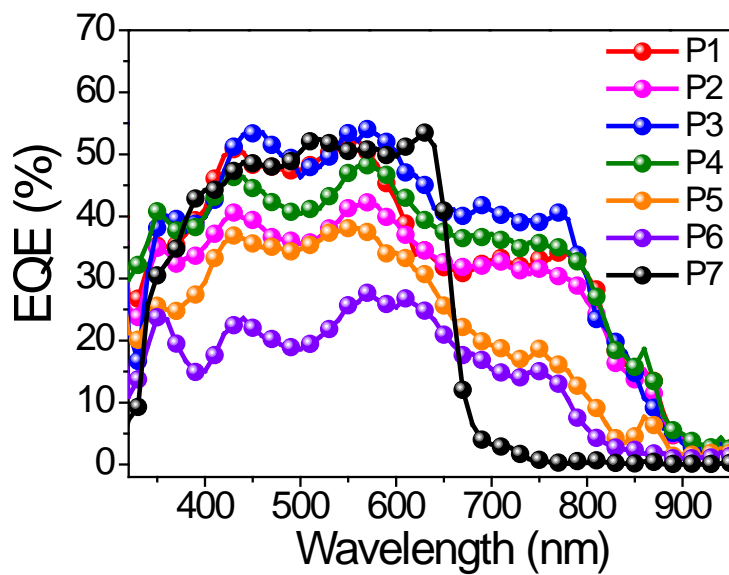


Figure S10. External quantum efficiencies (EQEs) of PSCs based on **P1-P7** devices under AM 1.5 illumination at 100 mW cm^{-2}